

On the spurious eigenvalues for a concentric sphere in BIEM

Jeng-Tzong Chen^{a,b,*}, Shing-Kai Kao^a, Ying-Te Lee^a, Yi-Jhou Lin^a

^a Department of Harbor and River Engineering, National Taiwan Ocean University, Keelung 20224, Taiwan

^b Department of Mechanical and Mechanical Engineering, National Taiwan Ocean University, Keelung 20224, Taiwan

ARTICLE INFO

Article history:

Received 12 November 2008

Received in revised form 23 July 2009

Accepted 3 August 2009

Available online 22 October 2009

Keywords:

Null-field integral equation

Degenerate kernel

Eigenproblem

Spurious eigenvalue

Singular value decomposition

ABSTRACT

In this paper, the null-field integral equation method is employed to study the occurring mechanism of spurious eigenvalues for a concentric sphere. By expanding the fundamental solution into degenerate kernels and expressing the boundary density in terms of spherical harmonics, all boundary integrals can be analytically determined. It is noted that our null-field integral formulation can locate the collocation point on the real boundary thanks to the degenerate kernel. In addition, the spurious eigenvalues are parasitized in the formulations while true eigensolutions are dependent on the boundary condition such as the Dirichlet or Neumann problem. By using the updating term and updating document of singular value decomposition (SVD) technique, true and spurious eigenvalues can be extracted out, respectively. Besides, true and spurious boundary eigenvectors are obtained in the right and left unitary vectors in the SVD structure of the influence matrices. This finding agrees with that of 2D cases.

Crown Copyright © 2009 Published by Elsevier Ltd. All rights reserved.

1. Introduction

The application of eigenanalysis is gradually increasing for vibration and acoustics. The demand for eigenanalysis calls for an efficient and reliable method of computation for eigenvalues and eigenmodes. Over the past three decades, several boundary element formulations had been employed to solve the eigenproblems [1,2], e.g., determinant searching method, internal cell method, dual reciprocity method, particular integral method and multiple reciprocity method. In this paper, we will focus on the determinant searching method with emphasis on spurious eigenvalues when using the BIEM for 3D problems with an inner cavity. Spurious and fictitious solutions stem from the problems of non-uniqueness solution which appear in different aspects in computational mechanics. First of all, the occurrence of hourglass modes in the finite element method (FEM) using the reduced integration stems from the rank deficiency [3]. Also, loss of divergence-free constraint for the incompressible elasticity results in spurious modes. On the other hand, while solving the differential equation by using the finite difference method (FDM), the spurious eigenvalue also appears due to discretization [4–6]. In the real-part BEM [7] or the MRM formulation [8–13], spurious eigensolutions occur in

solving eigenproblems. Even though the complex-valued kernel is adopted, the spurious eigensolution also occurs for the multiply-connected problem [14,15] as well as the appearance of fictitious frequency for the exterior acoustics [16]. Spurious eigenvalues in the MFS for 3D problems were also studied by Tsai et al. [17]. In this paper, a simple case of 3D concentric sphere will be demonstrated to see how spurious eigensolutions occur and how they are suppressed by using singular value decomposition (SVD).

In the recent years, the SVD technique has been applied to solve problems of fictitious frequency [16] and continuum mechanics [18]. Two ideas, namely updating term and updating document [1,16], were successfully applied to extract the true and spurious solutions, respectively. In this paper, the three-dimensional eigenproblem of a concentric sphere is studied in both numerical and analytical ways. Owing to the introduction of degenerate kernel, the collocation point can be located exactly on the real boundary. Besides, true and spurious equations can be found by using the null-field integral equation in conjunction with degenerate kernels and spherical harmonics for a concentric sphere. Surface distributions of the inner and outer boundaries can be expanded in terms of spherical harmonics. Since a spurious eigenvalue is embedded in the numerical method and has no physical meaning, the remedies, SVD updating term and SVD updating document, are used to extract or filter out true and spurious eigenvalues, respectively. Finally, an example with various boundary conditions is utilized to validate the present approach by using singular and hypersingular formulations.

* Corresponding author. Address: Department of Harbor and River Engineering, National Taiwan Ocean University, Keelung 20224, Taiwan. Tel.: +886 2 24622192x6177; fax: +886 2 24632375.

E-mail address: jtchen@mail.ntou.edu.tw (J.-T. Chen).

2. Null-field integral equation formulation

2.1. Problem statements

The governing equation for the eigenproblem of a concentric sphere is the Helmholtz equation as follows:

$$(\nabla^2 + k^2)u(x) = 0, \quad x \in D, \tag{1}$$

where ∇^2 , k and D are the Laplacian operator, the wave number and the domain of interest, respectively. The concentric sphere is depicted in Fig. 1. The inner and outer radii are a and b , respectively.

2.2. Dual null-field integral formulation—the conventional version

The dual boundary integral formulation [6] for the domain point is shown below:

$$4\pi u(x) = \int_B T(s, x)u(s)dB(s) - \int_B U(s, x) \frac{\partial u(s)}{\partial n_s} dB(s), \quad x \in D, \tag{2}$$

$$4\pi \frac{\partial u(x)}{\partial n_x} = \int_B M(s, x)u(s)dB(s) - \int_B L(s, x) \frac{\partial u(s)}{\partial n_s} dB(s), \quad x \in D, \tag{3}$$

where x and s are the field and source points, respectively, B is the boundary, n_x and n_s denote the outward normal vector at the field point and the source point, respectively, and the kernel function $U(s, x)$ is the fundamental solution which satisfies

$$(\nabla^2 + k^2)U(s, x) = 4\pi\delta(x - s), \tag{4}$$

where δ is the Dirac-delta function. The other kernel functions can be obtained as

$$T(s, x) = \frac{\partial U(s, x)}{\partial n_s}, \tag{5}$$

$$L(s, x) = \frac{\partial U(s, x)}{\partial n_x}, \tag{6}$$

$$M(s, x) = \frac{\partial^2 U(s, x)}{\partial n_s \partial n_x}. \tag{7}$$

If the collocation point x is on the boundary, the dual boundary integral equations for the boundary point can be obtained as follows:

$$2\pi u(x) = C.P.V. \int_B T(s, x)u(s)dB(s) - R.P.V. \int_B U(s, x) \frac{\partial u(s)}{\partial n_s} dB(s), \quad x \in B, \tag{8}$$

$$2\pi \frac{\partial u(x)}{\partial n_x} = H.P.V. \int_B M(s, x)u(s)dB(s) - C.P.V. \int_B L(s, x) \frac{\partial u(s)}{\partial n_s} dB(s), \quad x \in B, \tag{9}$$

where *R.P.V.*, *C.P.V.* and *H.P.V.* are the Riemann principal value, the Cauchy principal value and the Hadamard (or called Mangler) prin-

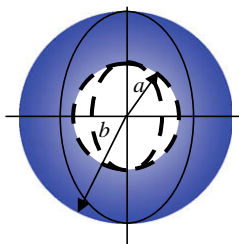


Fig. 1. A concentric sphere.

cipal value, respectively. By collocating x outside the domain, we obtain the null-field integral equation as shown below:

$$0 = \int_B T(s, x)u(s)dB(s) - \int_B U(s, x) \frac{\partial u(s)}{\partial n_s} dB(s), \quad x \in D^c, \tag{10}$$

$$0 = \int_B M(s, x)u(s)dB(s) - \int_B L(s, x) \frac{\partial u(s)}{\partial n_s} dB(s), \quad x \in D^c, \tag{11}$$

where D^c denotes the complementary domain.

2.3. Dual null-field integral formulation—the present version

By introducing the degenerate kernels, the collocation points can be located on the real boundary free of facing the principal value by using the bump contour approach. Therefore, the representations of integral equations including the boundary point can be written as

$$4\pi u(x) = \int_B T(s, x)u(s)dB(s) - \int_B U(s, x) \frac{\partial u(s)}{\partial n_s} dB(s), \quad x \in D \cup B, \tag{12}$$

$$4\pi \frac{\partial u(x)}{\partial n_x} = \int_B M(s, x)u(s)dB(s) - \int_B L(s, x) \frac{\partial u(s)}{\partial n_s} dB(s), \quad x \in D \cup B, \tag{13}$$

and

$$0 = \int_B T(s, x)u(s)dB(s) - \int_B U(s, x) \frac{\partial u(s)}{\partial n_s} dB(s), \quad x \in D^c \cup B, \tag{14}$$

$$0 = \int_B M(s, x)u(s)dB(s) - \int_B L(s, x) \frac{\partial u(s)}{\partial n_s} dB(s), \quad x \in D^c \cup B, \tag{15}$$

once the kernel is expressed in terms of an appropriate degenerate form. It is found that the collocation point is categorized to three positions, domain (Eqs. (2) and (3)), boundary (Eqs. (8) and (9)) and complementary domain (Eqs. (10) and (11)) in the conventional formulation. After using the degenerate kernel for the null-field BIEM, both Eqs. (12)–(15) can contain the boundary point. The resulted linear algebraic systems derived from Eqs. (12)–(15) are the same [19], i.e. we can move to the boundary either from the domain point or null-field point. The main reason can be found from the Appendix A to see how jump terms appear.

2.4. Expansions of the fundamental solution and boundary density

The fundamental solution as previously mentioned is

$$U(s, x) = -\frac{e^{-ikr}}{r}, \tag{16}$$

where $r = |s - x|$ is the distance between the source point and the field point and i is the imaginary number with $i^2 = -1$. To fully utilize the property of spherical geometry, the mathematical tools, degenerate (separable or finite rank) kernel and spherical harmonics, are utilized for the analytically calculating the boundary integrals.

2.4.1. Degenerate kernel for fundamental solutions

In the spherical coordinates, the field point (x) and source point (s) can be expressed as $x = (\rho, \phi, \theta)$ and $s = (\bar{\rho}, \bar{\phi}, \bar{\theta})$, respectively. By employing the addition theorem for separating the source point and field point, the kernel functions, $U(s, x)$, $T(s, x)$, $L(s, x)$ and $M(s, x)$, are expanded in terms of degenerate kernel as shown below:

$$U(s, x) = \begin{cases} U^i(s, x) = ik \sum_{n=0}^{\infty} (2n+1) \sum_{m=0}^n \varepsilon_m \frac{(n-m)!}{(n+m)!} \cos(m(\phi - \bar{\phi})) \\ \quad P_n^m(\cos \theta) P_n^m(\cos \bar{\theta}) j_n(k\rho) h_n^{(2)}(k\bar{\rho}), \quad \bar{\rho} \geq \rho, \\ U^e(s, x) = ik \sum_{n=0}^{\infty} (2n+1) \sum_{m=0}^n \varepsilon_m \frac{(n-m)!}{(n+m)!} \cos(m(\phi - \bar{\phi})) \\ \quad P_n^m(\cos \theta) P_n^m(\cos \bar{\theta}) j_n(k\bar{\rho}) h_n^{(2)}(k\rho), \quad \rho > \bar{\rho}, \end{cases} \quad (17)$$

$$T(s, x) = \begin{cases} T^i(s, x) = ik^2 \sum_{n=0}^{\infty} (2n+1) \sum_{m=0}^n \varepsilon_m \frac{(n-m)!}{(n+m)!} \cos(m(\phi - \bar{\phi})) \\ \quad P_n^m(\cos \theta) P_n^m(\cos \bar{\theta}) j_n(k\rho) h_n^{(2)}(k\bar{\rho}), \quad \bar{\rho} > \rho, \\ T^e(s, x) = ik^2 \sum_{n=0}^{\infty} (2n+1) \sum_{m=0}^n \varepsilon_m \frac{(n-m)!}{(n+m)!} \cos(m(\phi - \bar{\phi})) \\ \quad P_n^m(\cos \theta) P_n^m(\cos \bar{\theta}) j_n'(k\bar{\rho}) h_n^{(2)}(k\rho), \quad \rho > \bar{\rho}, \end{cases} \quad (18)$$

$$L(s, x) = \begin{cases} L^i(s, x) = ik^2 \sum_{n=0}^{\infty} (2n+1) \sum_{m=0}^n \varepsilon_m \frac{(n-m)!}{(n+m)!} \cos(m(\phi - \bar{\phi})) \\ \quad P_n^m(\cos \theta) P_n^m(\cos \bar{\theta}) j_n'(k\rho) h_n^{(2)}(k\bar{\rho}), \quad \bar{\rho} > \rho, \\ L^e(s, x) = ik^2 \sum_{n=0}^{\infty} (2n+1) \sum_{m=0}^n \varepsilon_m \frac{(n-m)!}{(n+m)!} \cos(m(\phi - \bar{\phi})) \\ \quad P_n^m(\cos \theta) P_n^m(\cos \bar{\theta}) j_n(k\bar{\rho}) h_n^{(2)}(k\rho), \quad \rho > \bar{\rho}, \end{cases} \quad (19)$$

$$M(s, x) = \begin{cases} M^i(s, x) = ik^3 \sum_{n=0}^{\infty} (2n+1) \sum_{m=0}^n \varepsilon_m \frac{(n-m)!}{(n+m)!} \cos(m(\phi - \bar{\phi})) \\ \quad P_n^m(\cos \theta) P_n^m(\cos \bar{\theta}) j_n'(k\rho) h_n^{(2)}(k\bar{\rho}), \quad \bar{\rho} \geq \rho, \\ M^e(s, x) = ik^3 \sum_{n=0}^{\infty} (2n+1) \sum_{m=0}^n \varepsilon_m \frac{(n-m)!}{(n+m)!} \cos(m(\phi - \bar{\phi})) \\ \quad P_n^m(\cos \theta) P_n^m(\cos \bar{\theta}) j_n'(k\bar{\rho}) h_n^{(2)}(k\rho), \quad \rho > \bar{\rho}, \end{cases} \quad (20)$$

where the superscripts “i” and “e” denote the interior and exterior regions, j_n and $h_n^{(2)}$ are the n th order spherical Bessel function of the first kind and the n th order spherical Hankel function of the second kind, respectively, P_n^m is the associated Legendre polynomial and ε_m is the Neumann factor,

$$\varepsilon_m = \begin{cases} 1, & m = 0, \\ 2, & m = 1, 2, \dots, \infty. \end{cases} \quad (21)$$

It is noted that U and M kernels in Eqs. (17) and (20) contain the equal sign of $\rho = \bar{\rho}$ while T and L kernels do not include the equal sign due to discontinuity in Eqs. (18) and (19). Besides, the potential across the boundary is also addressed here. For 2D Laplace and Helmholtz equations, the continuous and jump behavior across the boundary were studied, respectively, in [20,21]. After using the Wronskian property of j_m and y_m , we have

$$W(j_m(k\bar{\rho}), y_m(k\bar{\rho})) = j_m(k\bar{\rho})y_m'(k\bar{\rho}) - j_m'(k\bar{\rho})y_m(k\bar{\rho}) = \frac{1}{k^2\bar{\rho}^2}, \quad (22)$$

where $h_m^{(2)}(k\bar{\rho}) = j_m(k\bar{\rho}) - iy_m(k\bar{\rho})$. The jump behavior is well captured by

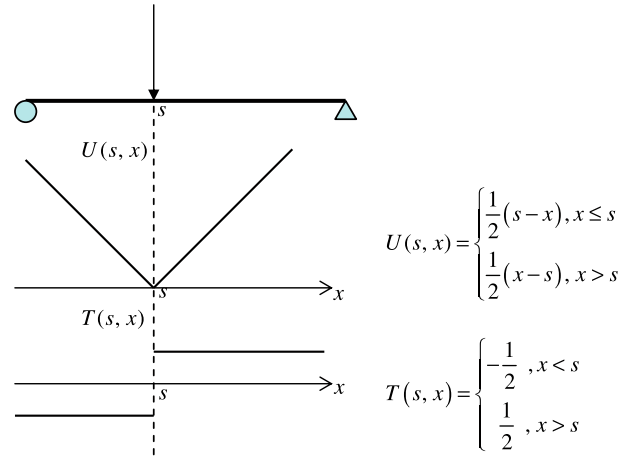


Fig. 2. Jump behavior for a rod case.

$$\int_0^{2\pi} \int_0^\pi [T^i(s, x) - T^e(s, x)] P_n^m(\cos \bar{\theta}) \cos(m\bar{\phi}) \bar{\rho}^2 \sin(\bar{\theta}) d\bar{\theta} d\bar{\phi} = -4\pi k P_n^m(\cos \theta) \cos(m\phi) \quad (23)$$

Similarly, the potentials due to L^i and L^e kernels are discontinuous across the boundary. For clarity, a detailed description is given in Appendix A. For simplicity, we also give a simple example by a rod case to show how the jump appears. The degenerate kernels are shown in Fig. 2.

2.4.2. Spherical harmonics for boundary densities

We used the spherical harmonics to approximate the boundary density and its normal derivative as expressed by

$$u(s) = \sum_{v=0}^{\infty} \sum_{w=0}^v A_{vw} P_v^w(\cos \bar{\theta}) \cos(w\bar{\phi}), \quad s \in B, \quad (24)$$

$$t(s) = \frac{\partial u(s)}{\partial n_s} = \sum_{v=0}^{\infty} \sum_{w=0}^v B_{vw} P_v^w(\cos \bar{\theta}) \cos(w\bar{\phi}), \quad s \in B, \quad (25)$$

where A_{vw} and B_{vw} are the unknown coefficients.

3. Null-field integral equation

In order to fully utilize the geometry of sphere boundary, the potential u and its normal derivative t can be approximated by employing the spherical harmonic functions. Therefore, the following expressions can be obtained

$$u_1(s) = \sum_{v=0}^{\infty} \sum_{w=0}^v A_{vw}^1 P_v^w(\cos \bar{\theta}) \cos(w\bar{\phi}), \quad s \in B_1, \quad (26)$$

$$u_2(s) = \sum_{v=0}^{\infty} \sum_{w=0}^v A_{vw}^2 P_v^w(\cos \bar{\theta}) \cos(w\bar{\phi}), \quad s \in B_2, \quad (27)$$

$$t_1(s) = \sum_{v=0}^{\infty} \sum_{w=0}^v B_{vw}^1 P_v^w(\cos \bar{\theta}) \cos(w\bar{\phi}), \quad s \in B_1, \quad (28)$$

$$t_2(s) = \sum_{v=0}^{\infty} \sum_{w=0}^v B_{vw}^2 P_v^w(\cos \bar{\theta}) \cos(w\bar{\phi}), \quad s \in B_2, \quad (29)$$

where A_{vw}^i and B_{vw}^i are the spherical coefficients on B_i ($i = 1, 2$). By substituting Eqs. (26)–(29) into the null-field integral equations and moving the null-field point to the boundary, we have

$$\begin{aligned}
 0 = & \int_0^{2\pi} \int_0^\pi \sum_{n=0}^\infty \sum_{m=0}^n \sum_{\nu=0}^\infty \sum_{w=0}^\nu ik^2 \varepsilon_m A_{\nu w}^1 (2n+1) \\
 & \frac{(n-m)!}{(n+m)!} j_n(k\rho) h_n^{(2)}(ka) P_n^m(\cos(\theta)) \cos(m(\phi - \bar{\phi})) \\
 & \cos(w\bar{\phi}) (P_n^m(\cos(\bar{\theta})) P_\nu^w(\cos(\bar{\theta})) \sin(\bar{\theta})) a^2 d\bar{\theta} d\bar{\phi} \\
 & - \int_0^{2\pi} \int_0^\pi \sum_{n=0}^\infty \sum_{m=0}^n \sum_{\nu=0}^\infty \sum_{w=0}^\nu ik \varepsilon_m B_{\nu w}^1 (2n+1) \\
 & \frac{(n-m)!}{(n+m)!} j_n(k\rho) h_n^{(2)}(ka) P_n^m(\cos(\theta)) \cos(m(\phi - \bar{\phi})) \\
 & \cos(w\bar{\phi}) (P_n^m(\cos(\bar{\theta})) P_\nu^w(\cos(\bar{\theta})) \sin(\bar{\theta})) a^2 d\bar{\theta} d\bar{\phi} \\
 & + \int_0^{2\pi} \int_0^\pi \sum_{n=0}^\infty \sum_{m=0}^n \sum_{\nu=0}^\infty \sum_{w=0}^\nu ik^2 \varepsilon_m A_{\nu w}^2 (2n+1) \\
 & \frac{(n-m)!}{(n+m)!} j_n(k\rho) h_n^{(2)}(kb) P_n^m(\cos(\theta)) \cos(m(\phi - \bar{\phi})) \\
 & \cos(w\bar{\phi}) (P_n^m(\cos(\bar{\theta})) P_\nu^w(\cos(\bar{\theta})) \sin(\bar{\theta})) b^2 d\bar{\theta} d\bar{\phi} \\
 & - \int_0^{2\pi} \int_0^\pi \sum_{n=0}^\infty \sum_{m=0}^n \sum_{\nu=0}^\infty \sum_{w=0}^\nu ik \varepsilon_m B_{\nu w}^2 (2n+1) \\
 & \frac{(n-m)!}{(n+m)!} j_n(k\rho) h_n^{(2)}(kb) P_n^m(\cos(\theta)) \cos(m(\phi - \bar{\phi})) \\
 & \cos(w\bar{\phi}) (P_n^m(\cos(\bar{\theta})) P_\nu^w(\cos(\bar{\theta})) \sin(\bar{\theta})) b^2 d\bar{\theta} d\bar{\phi}. \tag{30}
 \end{aligned}$$

When the field point is located on the outer boundary B_2 , we have

$$\begin{aligned}
 0 = & \int_0^{2\pi} \int_0^\pi \sum_{n=0}^\infty \sum_{m=0}^n \sum_{\nu=0}^\infty \sum_{w=0}^\nu ik^2 \varepsilon_m A_{\nu w}^1 (2n+1) \\
 & \frac{(n-m)!}{(n+m)!} j_n(ka) h_n^{(2)}(k\rho) P_n^m(\cos(\theta)) \cos(m(\phi - \bar{\phi})) \\
 & \cos(w\bar{\phi}) (P_n^m(\cos(\bar{\theta})) P_\nu^w(\cos(\bar{\theta})) \sin(\bar{\theta})) a^2 d\bar{\theta} d\bar{\phi} \\
 & - \int_0^{2\pi} \int_0^\pi \sum_{n=0}^\infty \sum_{m=0}^n \sum_{\nu=0}^\infty \sum_{w=0}^\nu ik \varepsilon_m B_{\nu w}^1 (2n+1) \\
 & \frac{(n-m)!}{(n+m)!} j_n(ka) h_n^{(2)}(k\rho) P_n^m(\cos(\theta)) \cos(m(\phi - \bar{\phi})) \\
 & \cos(w\bar{\phi}) (P_n^m(\cos(\bar{\theta})) P_\nu^w(\cos(\bar{\theta})) \sin(\bar{\theta})) a^2 d\bar{\theta} d\bar{\phi} \\
 & + \int_0^{2\pi} \int_0^\pi \sum_{n=0}^\infty \sum_{m=0}^n \sum_{\nu=0}^\infty \sum_{w=0}^\nu ik^2 \varepsilon_m A_{\nu w}^2 (2n+1) \\
 & \frac{(n-m)!}{(n+m)!} j_n(kb) h_n^{(2)}(k\rho) P_n^m(\cos(\theta)) \cos(m(\phi - \bar{\phi})) \\
 & \cos(w\bar{\phi}) (P_n^m(\cos(\bar{\theta})) P_\nu^w(\cos(\bar{\theta})) \sin(\bar{\theta})) b^2 d\bar{\theta} d\bar{\phi} \\
 & - \int_0^{2\pi} \int_0^\pi \sum_{n=0}^\infty \sum_{m=0}^n \sum_{\nu=0}^\infty \sum_{w=0}^\nu ik \varepsilon_m B_{\nu w}^2 (2n+1) \\
 & \frac{(n-m)!}{(n+m)!} j_n(kb) h_n^{(2)}(k\rho) P_n^m(\cos(\theta)) \cos(m(\phi - \bar{\phi})) \\
 & \cos(w\bar{\phi}) (P_n^m(\cos(\bar{\theta})) P_\nu^w(\cos(\bar{\theta})) \sin(\bar{\theta})) b^2 d\bar{\theta} d\bar{\phi}. \tag{31}
 \end{aligned}$$

For the Dirichlet problem, Eqs. (30) and (31) can be reduced to

$$\begin{aligned}
 0 = & \sum_{n=0}^\infty \sum_{m=0}^n a^2 k B_{nm}^1 j_n(ka) h_n^{(2)}(ka) P_n^m(\cos(\theta)) \cos(m\phi) \\
 & + \sum_{n=0}^\infty \sum_{m=0}^n b^2 k B_{nm}^2 j_n(ka) h_n^{(2)}(kb) P_n^m(\cos(\theta)) \cos(m\phi), \tag{32}
 \end{aligned}$$

$$\begin{aligned}
 0 = & \sum_{n=0}^\infty \sum_{m=0}^n a^2 k B_{nm}^1 j_n(ka) h_n^{(2)}(kb) P_n^m(\cos(\theta)) \cos(m\phi) \\
 & + \sum_{n=0}^\infty \sum_{m=0}^n b^2 k B_{nm}^2 j_n(kb) h_n^{(2)}(kb) P_n^m(\cos(\theta)) \cos(m\phi). \tag{33}
 \end{aligned}$$

According to Eqs. (32) and (33), the spherical coefficients, B_{nm}^1 and B_{nm}^2 , satisfy the relation as follows:

$$B_{nm}^2 = - \frac{a^2 j_n(ka) h_n^{(2)}(ka)}{b^2 j_n(kb) h_n^{(2)}(kb)} B_{nm}^1, \tag{34}$$

$$B_{nm}^2 = - \frac{a^2 j_n'(ka) h_n^{(2)}(kb)}{b^2 j_n'(kb) h_n^{(2)}(kb)} B_{nm}^1. \tag{35}$$

To seek the nontrivial data for the spherical coefficients B_{nm}^1 and B_{nm}^2 , we obtain the eigenequation:

$$j_n(ka) h_n^{(2)}(kb) [j_n(kb) h_n^{(2)}(ka) - j_n(ka) h_n^{(2)}(kb)] = 0 \tag{36}$$

For the Neumann problem, the Eqs. (30) and (31) are reduced to

$$0 = \sum_{n=0}^\infty \sum_{m=0}^n a^2 A_{nm}^1 j_n(ka) h_n^{(2)}(ka) + \sum_{n=0}^\infty \sum_{m=0}^n b^2 A_{nm}^2 j_n(ka) h_n^{(2)}(kb), \tag{37}$$

$$0 = \sum_{n=0}^\infty \sum_{m=0}^n a^2 A_{nm}^1 j_n'(ka) h_n^{(2)}(kb) + \sum_{n=0}^\infty \sum_{m=0}^n b^2 A_{nm}^2 j_n'(kb) h_n^{(2)}(kb). \tag{38}$$

According to Eqs. (37) and (38), the spherical coefficients A_{nm}^1 and A_{nm}^2 satisfy the relations:

$$A_{nm}^2 = - \frac{a^2 j_n(ka) h_n^{(2)}(ka)}{b^2 j_n(ka) h_n^{(2)}(kb)} A_{nm}^1, \tag{39}$$

$$A_{nm}^2 = - \frac{a^2 j_n'(ka) h_n^{(2)}(kb)}{b^2 j_n'(kb) h_n^{(2)}(kb)} A_{nm}^1. \tag{40}$$

To seek the nontrivial data for the spherical coefficients A_{nm}^1 and A_{nm}^2 , we obtain the eigenequation:

$$j_n(ka) h_n^{(2)}(kb) [j_n'(kb) h_n^{(2)}(ka) - j_n'(ka) h_n^{(2)}(kb)] = 0. \tag{41}$$

According to Eqs. (36) and (41), the spurious eigenequation of the singular formulation is $j_n(ka) = 0$, which is also the true eigenequation of the sphere of radius a with the fixed boundary condition. The latter parts in the bracket of Eqs. (36) and (41) are the true eigenequations,

$$j_n(kb) h_n^{(2)}(ka) - j_n(ka) h_n^{(2)}(kb) = 0 \quad \text{for the Dirichlet problem} \tag{42}$$

$$j_n'(kb) h_n^{(2)}(ka) - j_n'(ka) h_n^{(2)}(kb) = 0 \quad \text{for the Neumann problem} \tag{43}$$

The spurious and true eigenequations of the concentric sphere subject to various boundary conditions are listed in Table 1. It is interesting to find that spurious eigenvalue of *UT* (singular) formulation results in trivial outer boundary modes for the fixed–fixed case. Besides, spurious eigenvalue of *LM* (hypersingular) formulation results in the trivial outer boundary modes of free–free case.

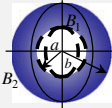
4. Proof of the existence for the spurious eigensolutions of the eccentric sphere

In order to prove that the spurious eigensolutions of a eccentric sphere satisfy the BIE by collocating the inner and outer boundary points, we first derive the true eigensolutions of a sphere subject to the Dirichlet boundary condition. Now, we consider the sphere with a radius a in the continuous system. By using the null-field integral equation and collocating the point on the boundary, we obtain the true eigenequation

$$j_n(ka) = 0, \tag{44}$$

and the corresponding true eigenmode is B_{nm} , where $\sum \sum |B_{nm}| \neq 0$. By collocating the point in the complementary domain ($x^c \in D^c$) as shown in Fig. 3, the null-field equation yields

Table 1
Eigensolutions and boundary modes for the concentric sphere subject to different boundary conditions.

	Solution	BC			
		Fixed–fixed $u_1 = u_2 = 0$	Free–fixed $t_1 = u_2 = 0$	Fixed–free $u_1 = t_2 = 0$	Free–free $t_1 = t_2 = 0$
UT formulation	True eigenequation	$j_n(ka)y_n(kb) - j_n(kb)y_n(ka) = 0$	$j'_n(ka)y_n(kb) - j'_n(kb)y'_n(ka) = 0$	$j_n(ka)y'_n(kb) - j'_n(kb)y_n(ka) = 0$	$j'_n(ka)y'_n(kb) - j'_n(kb)y'_n(ka) = 0$
	Spurious eigenequation	$j_n(ka) = 0$	$j'_n(ka) = 0$	$j_n(ka) = 0$	$j_n(ka) = 0$
	Inner boundary mode	$\sum \sum B_{nm} \neq 0$	$\sum \sum A_{nm} \neq 0$	$\sum \sum B_{nm} \neq 0$	$\sum \sum A_{nm} \neq 0$
	Outer boundary mode	$B_{nm}^2 = \frac{a^2 j_n(ka)}{b^2 j_n(kb)} B_{nm}^1$	$B_{nm}^2 = \frac{a^2 j'_n(ka)}{b^2 j'_n(kb)} A_{nm}^1$	$A_{nm}^2 = \frac{a^2 j_n(ka)}{b^2 j_n(kb)} B_{nm}^1$	$A_{nm}^2 = \frac{a^2 j'_n(ka)}{b^2 j'_n(kb)} A_{nm}^1$
LM formulation	True eigenequation	$j_n(ka)y_n(kb) - j_n(kb)y_n(ka) = 0$	$j'_n(ka)y_n(kb) - j'_n(kb)y'_n(ka) = 0$	$j_n(ka)y'_n(kb) - j'_n(kb)y_n(ka) = 0$	$j'_n(ka)y'_n(kb) - j'_n(kb)y'_n(ka) = 0$
	Spurious eigenequation	$j'_n(ka) = 0$	$j'_n(ka) = 0$	$j'_n(ka) = 0$	$j'_n(ka) = 0$
	Inner boundary mode	$\sum \sum B_{nm} \neq 0$	$\sum \sum A_{nm} \neq 0$	$\sum \sum B_{nm} \neq 0$	$\sum \sum A_{nm} \neq 0$
	Outer boundary mode	$B_{nm}^2 = \frac{a^2 j_n(ka)}{b^2 j_n(kb)} B_{nm}^1$	$B_{nm}^2 = \frac{a^2 j'_n(ka)}{b^2 j'_n(kb)} A_{nm}^1$	$A_{nm}^2 = \frac{a^2 j_n(ka)}{b^2 j_n(kb)} B_{nm}^1$	$A_{nm}^2 = \frac{a^2 j'_n(ka)}{b^2 j'_n(kb)} A_{nm}^1$

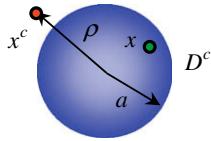


Fig. 3. Collocation point on the sphere boundary from the null-field point ($\rho = a^+$).

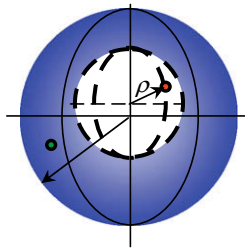


Fig. 4. Collocation point of the eccentric sphere ($\rho = a^-$).

$$0 = \int_{B_1} U^e(s, x^c) t(s) dB(s), \quad x^c \in D^c. \tag{45}$$

We can obtain the null-field response for x^c as shown below

$$B_{nm}^1 j_n(ka) h_n^{(2)}(ka^+) P_n^m(\cos(\theta)) \cos(m\phi) = 0, \tag{46}$$

where n and m belong to nature number and k satisfies Eq. (44).

Secondly, we consider the spherical case with the fixed-fixed boundary condition as shown in Fig. 4. By selecting a nontrivial inner boundary mode for the boundary mode and trivial outer boundary mode, we have $j_n(ka) = 0$ and

$$\begin{Bmatrix} B_{nm}^1 \\ B_{nm}^2 \end{Bmatrix} = \begin{Bmatrix} B_{nm} \\ 0 \end{Bmatrix} \tag{47}$$

This indicates that spurious eigenevalues of $j_n(ka) = 0$ and the non-trivial boundary mode of Eq. (47) satisfy Eqs. (32) and (33) due to $U^i(s, a^-) = U^e(s, a^+)$. Therefore, spurious eigenevalues in conjunction with the trivial outer boundary mode happen to be the true eigenvalue of the domain bounded by the inner boundary. Similarly, the

concentric sphere subjected to the Neumann boundary condition by using the hypersingular formulation results in the trivial outer boundary mode.

5. SVD technique for extracting out true and spurious eigenevalues by using updating terms and updating documents

5.1. Method of extracting the true eigensolutions (updating terms)

SVD technique is an important tool in the linear algebra. The matrix $[A]$ with a dimension M by N can be decomposed into a product of the unitary matrix $[\Phi]$ (M by M), the diagonal matrix $[\Sigma]$ (M by N) with positive or zero elements, and the unitary matrix $[\Psi]$ (N by N) as follows:

$$[A]_{M \times N} = [\Phi]_{M \times M} [\Sigma]_{M \times N} [\Psi]_{N \times N}^H, \tag{48}$$

where the superscript “ H ” is the Hermitian operator, $[\Phi]$ and $[\Psi]$ are both unitary matrices that their column vectors which satisfy

$$\tilde{\phi}_i^H \cdot \tilde{\phi}_j = \delta_{ij}, \tag{49}$$

$$\tilde{\psi}_i^H \cdot \tilde{\psi}_j = \delta_{ij}, \tag{50}$$

in which $[\Phi]^H [\Phi] = [I]_{M \times M}$ and $[\Psi]^H [\Psi] = [I]_{N \times N}$. For the eigenproblem, we can obtain a nontrivial solution for the homogeneous system from a column vector $\{\psi_i\}$ of $[\Psi]$ when the singular value (σ_i) is zero. For the BIEM, we have

Singular formulation (UT method)

$$[T^e]\{u\} = [U^e]\{t\} = \{0\}, \tag{51}$$

Hypersingular formulation (LM method)

$$[M^e]\{u\} = [L^e]\{t\} = \{0\}, \tag{52}$$

where $\{u\}$ and $\{t\}$ are the boundary excitations. For the Dirichlet problem, Eqs. (51) and (52) can be combined to have

$$\begin{Bmatrix} U^e \\ L^e \end{Bmatrix} \{t\} = \{0\}. \tag{53}$$

By using the SVD technique, the two submatrices in Eqs. (51) and (52) can be decomposed into

$$[\mathbf{U}^e] = [\Phi^{(U)}][\Sigma^{(U)}][\Psi^{(U)H}] \text{ or } [\mathbf{U}^e] = \sum_j \sigma_j^{(U)} \{\phi_j^{(U)}\} \{\psi_j^{(U)}\}^H, \quad (54)$$

$$[\mathbf{L}^e] = [\Phi^{(L)}][\Sigma^{(L)}][\Psi^{(L)H}] \text{ or } [\mathbf{L}^e] = \sum_j \sigma_j^{(L)} \{\phi_j^{(L)}\} \{\psi_j^{(L)}\}^H, \quad (55)$$

where the superscripts, (U) and (L), denote the corresponding matrices. For the linear algebraic system, {t} is a column vector of {ψ_i} in the matrix [Ψ] corresponding to the zero singular value (σ_i = 0). By setting {t} as a vector of {ψ_i} in the right unitary matrix for the true eigenvalue k_t, Eqs. (51) and (52) reduce to

$$[\mathbf{U}^e(k_t)]\{\psi_i\} = \{0\}, \quad (56)$$

$$[\mathbf{L}^e(k_t)]\{\psi_i\} = \{0\}. \quad (57)$$

According to Eqs. (54)–(57), we have

$$\sigma_j^{(U)}\{\phi_j^{(U)}\} = \{0\}, \quad (58)$$

$$\sigma_j^{(L)}\{\phi_j^{(L)}\} = \{0\}. \quad (59)$$

We can easily extract out the true eigenvalues, σ_j^(U) = σ_j^(L) = {0}, since there exists the same eigensolution ({t} = {ψ_i}) for the

Dirichlet problem by using Eqs. (53) or (56) and (58). In a similar way, Eqs. (51) and (52) can be combined to have

$$\begin{bmatrix} \mathbf{T}^e(k_t) \\ \mathbf{M}^e(k_t) \end{bmatrix} \{u\} = \{0\}, \quad (60)$$

for the Neumann problem. We can easily extract out the true eigenvalues for the Neumann problem with respect to the jth zero singular values of σ_j^(T) = σ_j^(M) = {0}.

5.2. Method of filtering out the spurious eugensolutions (updating documents)

By employing the LM formulation in the direct BEM, we have

$$[\mathbf{M}^e]\{u\} = [\mathbf{L}^e]\{t\} = \{p\}. \quad (61)$$

Since the spurious eigenvalue k_s is embedded in both the Dirichlet and Neumann problems, we have

$$\{p\}^H \{\phi_i\} = \{0\}, \quad (62)$$

where {φ_i} satisfies

Table 2a
SVD structure of the four influence matrices for the Dirichlet and Neumann problems in the case of true eigenvalue.

	Dirichlet problem ($k = k_r^D$)		Neumann problem ($k = k_r^N$)					
True eigenvalue k_r (k_r^D, k_r^N)	$[\Phi^U] \begin{bmatrix} 0 & & \\ & \ddots & \\ & & \phi_1^D \dots \end{bmatrix}^H$	$[\Phi^T][\Sigma^T][\Psi^T]^H$	$[\Phi^U][\Sigma^U][\Psi^U]^H$	$[\Phi^T] \begin{bmatrix} 0 & & \\ & \ddots & \\ & & \phi_1^N \dots \end{bmatrix}^H$				
	$[\Phi^L] \begin{bmatrix} 0 & & \\ & \ddots & \\ & & \phi_1^D \dots \end{bmatrix}^H$	$[\Phi^M][\Sigma^M][\Psi^M]^H$	$[\Phi^L][\Sigma^L][\Psi^L]^H$	$[\Phi^M] \begin{bmatrix} 0 & & \\ & \ddots & \\ & & \phi_1^N \dots \end{bmatrix}^H$				
	<div style="display: flex; align-items: center; justify-content: center;"> <div style="margin-right: 10px;">The same ϕ_1^D</div> <div style="border: 1px solid black; padding: 5px;"> <table style="border-collapse: collapse;"> <tr><td style="padding: 2px 5px;">U</td><td style="padding: 2px 5px;">T</td></tr> <tr><td style="padding: 2px 5px;">L</td><td style="padding: 2px 5px;">M</td></tr> </table> </div> <div style="margin-left: 10px;">The same ϕ_1^N</div> </div>		U	T	L	M		
U	T							
L	M							

where k_r^D and k_r^N denotes the true eigenvalues for the Dirichlet and Neumann problems, respectively.

Table 2b
SVD structure of the four influence matrices by using the UT singular formulation and LM hypersingular formulation in the case of spurious eigenvalue.

	UT singular formulation ($k = k_s^{UT}$)		LM hypersingular formulation ($k = k_s^{LM}$)				
	Dirichlet	Neumann	Dirichlet	Neumann			
Spurious eigenvalue k_s (k_s^{UT}, k_s^{LM})	$[\phi_1^{UT} \dots] \begin{bmatrix} 0 & & \\ & \ddots & \\ & & \Psi_{UT}^D \end{bmatrix}^H$	$[\phi_1^{UT} \dots] \begin{bmatrix} 0 & & \\ & \ddots & \\ & & \Psi_{UT}^N \end{bmatrix}^H$	$[\phi_1^{LM} \dots] \begin{bmatrix} 0 & & \\ & \ddots & \\ & & \Psi_{LM}^D \end{bmatrix}^H$	$[\phi_1^{LM} \dots] \begin{bmatrix} 0 & & \\ & \ddots & \\ & & \Psi_{LM}^N \end{bmatrix}^H$			
	<div style="display: flex; align-items: center; justify-content: center;"> <div style="margin-right: 10px;">The same ϕ_1^{UT}</div> <div style="border: 1px solid black; padding: 5px;"> <table style="border-collapse: collapse;"> <tr><td style="padding: 2px 5px;">U</td><td style="padding: 2px 5px;">T</td></tr> </table> </div> </div>		U	T	<div style="display: flex; align-items: center; justify-content: center;"> <div style="margin-right: 10px;">The same ϕ_1^{LM}</div> <div style="border: 1px solid black; padding: 5px;"> <table style="border-collapse: collapse;"> <tr><td style="padding: 2px 5px;">L</td><td style="padding: 2px 5px;">M</td></tr> </table> </div> </div>		L
U	T						
L	M						

where k_s^{UT} and k_s^{LM} denotes the spurious eigenvalues by using UT singular and LM hypersingular formulation, respectively.

$$[\mathbf{L}^e(k_s)]^H \{\phi_i\} = \{0\} \quad \text{for the Dirichlet problem,} \quad (63)$$

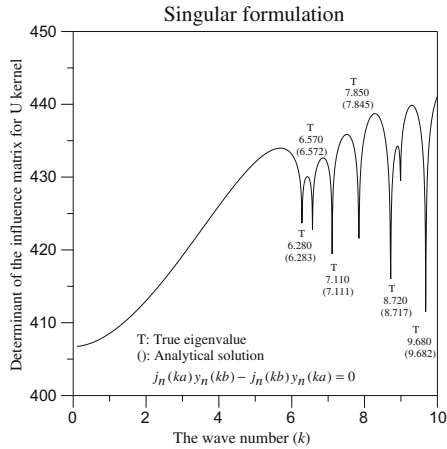
$$[\mathbf{M}^e(k_s)]^H \{\phi_i\} = \{0\} \quad \text{for the Neumann problem,} \quad (64)$$

according to the Fredholm alternative theorem. By substituting Eq. (61) into Eqs. (62)–(64), we have

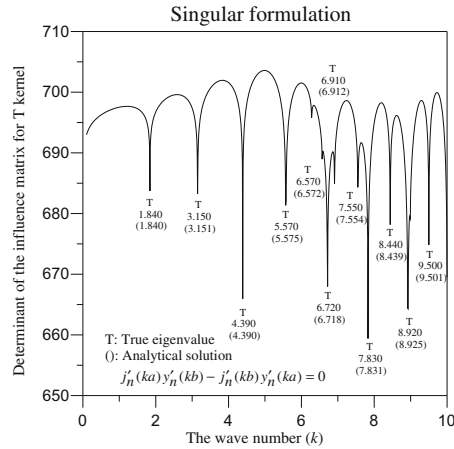
$$\{u\}^H [\mathbf{M}^e(k_s)]^H \{\phi_i\} = \{0\} \quad \text{for the Dirichlet problem,} \quad (65)$$

$$\{t\}^H [\mathbf{L}^e(k_s)]^H \{\phi_i\} = \{0\} \quad \text{for the Neumann problem.} \quad (66)$$

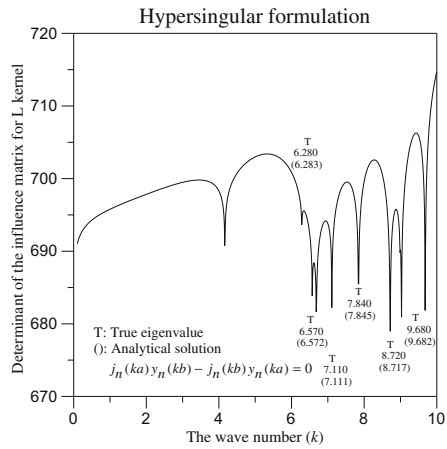
Since $\{u\}$ and $\{t\}$ can be arbitrary boundary excitation for the Dirichlet problem and Neumann problem, respectively, this yields



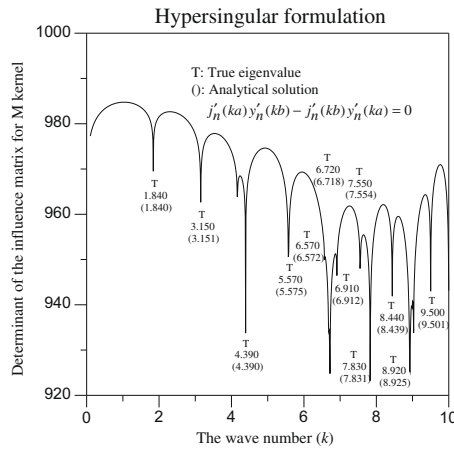
(a) Determinant versus the wave number by using the singular formulation for the Dirichlet condition.



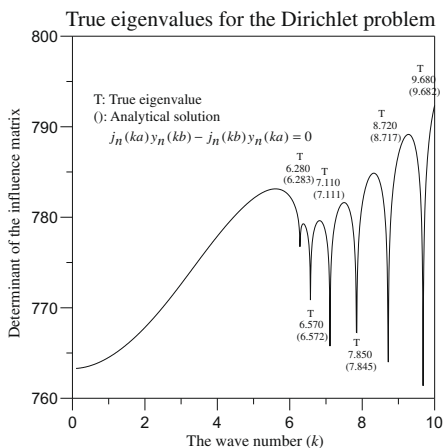
(d) Determinant versus the wave numbers by using the singular formulation for the Neumann condition.



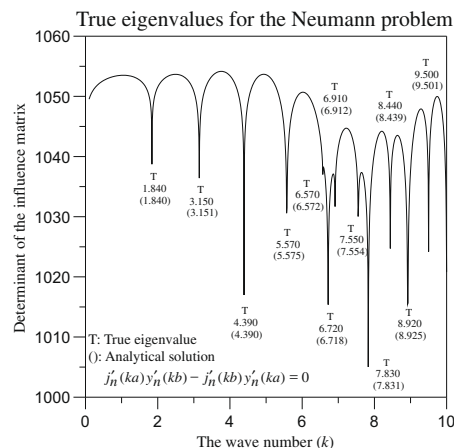
(b) Determinant versus the wave number by using the hypersingular formulation for the Dirichlet condition.



(e) Determinant versus the wave number by using the hypersingular formulation for the Neumann condition.

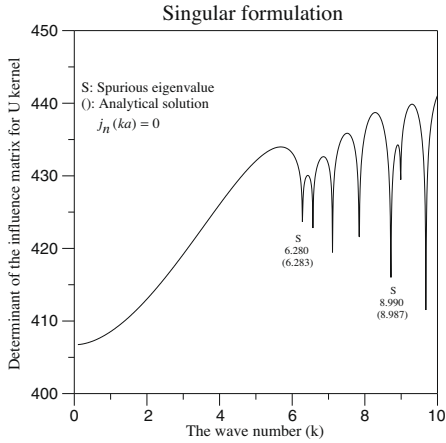


(c) Extraction of true eigenvalues for the Dirichlet problem by using the SVD updating terms.

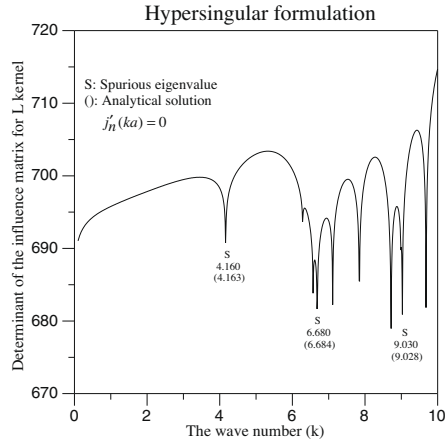


(f) Extraction of true eigenvalues for the Neumann problem by using the SVD updating terms.

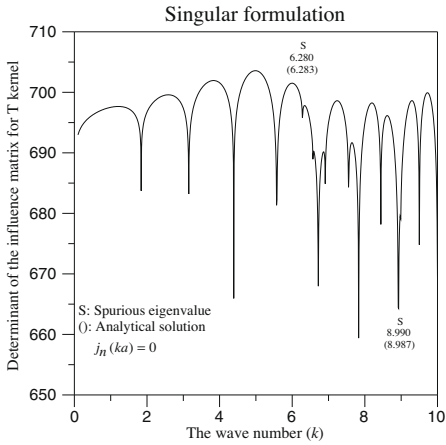
Fig. 5. True eigenvalues for a concentric sphere by using the SVD updating terms ($a = 0.5$ and $b = 1.0$).



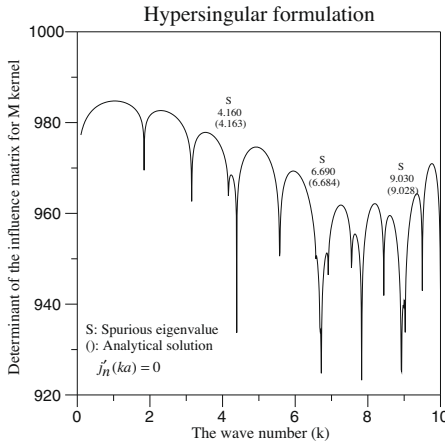
(a) Determinant versus the wave number by using the singular formulation subject to the Dirichlet condition.



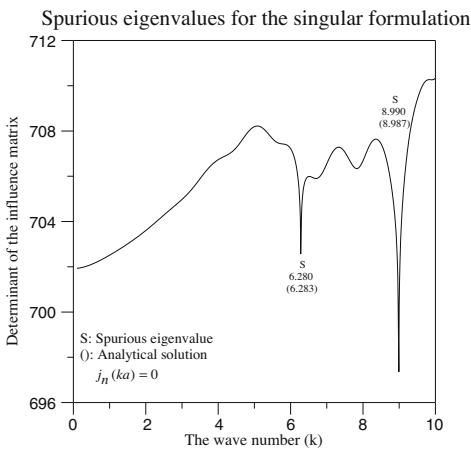
(d) Determinant versus the wave number by using the hypersingular formulation subject to the Dirichlet condition.



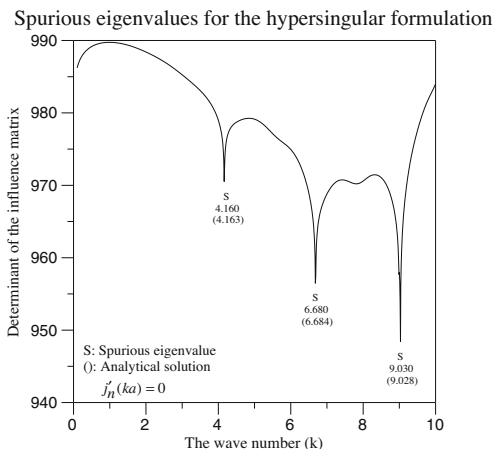
(b) Determinant versus the wave number by using the singular formulation subject to the Neumann condition.



(e) Determinant versus the wave number by using the hypersingular formulation subject to the Neumann condition.



(c) Extraction of the spurious eigenvalues for the singular formulation by using the SVD updating document.



(f) Extraction of the spurious eigenvalues for the hypersingular formulation by using the SVD updating document.

Fig. 6. Extraction of spurious eigenvalues for a concentric sphere by using the SVD updating documents ($a = 0.5$ and $b = 1.0$).

$$[\mathbf{M}^e(k_s)]^H \{\phi_i\} = \{0\} \quad \text{for the Dirichlet problem,} \quad (67)$$

$$[\mathbf{L}^e(k_s)]^H \{\phi_i\} = \{0\} \quad \text{for the Neumann problem.} \quad (68)$$

By combining Eq. (63) with Eq. (67) for the Dirichlet problem, we have

$$\begin{bmatrix} \mathbf{L}^{e_i H} \\ \mathbf{M}^{e_i H} \end{bmatrix} \{\phi_i\} = \{0\} \quad \text{or} \quad \{\phi_i\}^H [\mathbf{L}^e \quad \mathbf{M}^e] = \{0\}. \quad (69)$$

It indicates that two matrices have the same spurious boundary mode $\{\phi_i\}$ corresponding to the i th zero singular values. By using the SVD technique, two matrices in Eq. (69) can be decomposed into

$$\mathbf{L}^{e_i H} = [\Psi^{(L)}][\Sigma^{(L)}][\Phi^{(L)}]^H \quad \text{or} \quad \mathbf{L}^e = \sum_j \sigma_j^{(L)} \{\psi_j^{(L)}\} \{\phi_j^{(L)}\}^H, \quad (70)$$

$$\mathbf{M}^{e_i H} = [\Psi^{(M)}][\Sigma^{(M)}][\Phi^{(M)}]^H \quad \text{or} \quad \mathbf{M}^e = \sum_j \sigma_j^{(M)} \{\psi_j^{(M)}\} \{\phi_j^{(M)}\}^H. \quad (71)$$

By substituting Eqs. (70) and (71) into Eqs. (65) and (66), we have

$$\sigma_j^{(L)} \{\psi_j^{(L)}\} = \{0\}, \quad (72)$$

$$\sigma_j^{(M)} \{\psi_j^{(M)}\} = \{0\}. \quad (73)$$

We can easily extract out the spurious eigenvalues since there exists the same spurious boundary mode $\{\phi_i\}$ corresponding the i th zero singular value, $\sigma_i^{(L)} = \sigma_i^{(M)} = 0$. Similarly, the spurious eigenvalue parasitized in the UT formulation can be obtained by using SVD updating documents. To summarize the SVD structure for the four influence matrices, Tables 2a and 2b show that the spurious and true boundary modes are imbedded in the left and right unitary vectors, respectively. Besides, the nontrivial interior boundary mode and trivial outer boundary mode are also given in Table 2b.

6. Illustrative examples and discussion

Case 1: A concentric sphere subject to the Dirichlet boundary condition ($\mathbf{u}_1 = \mathbf{u}_2 = \mathbf{0}$) using the present approach.

A concentric case with radii a and b ($a = 0.5$ m and $b = 1.0$ m) is shown in Fig. 1. The analytical solution can be obtained by using the null-filed integral formulation, degenerate kernel and spherical harmonics. The common drop locations in Fig. 5a and b indicate the true eigenvalues. We employ the SVD updating term $\begin{bmatrix} U \\ L \end{bmatrix}$ to extract the true eigenvalues for the Dirichlet problem as shown in Fig. 5c. It is found that all the spurious eigenvalues are filtered out. The results agree well with the previous solutions.

Case 2: A concentric sphere subject to the Neumann boundary condition ($\mathbf{t}_1 = \mathbf{t}_2 = \mathbf{0}$) using the present approach.

Similarly, the common drop locations in Fig. 5d and e indicate the true eigenvalues. Extraction of true eigenvalues by using the SVD updating term $\begin{bmatrix} T \\ M \end{bmatrix}$ is shown in Fig. 5f. The common drop

locations in Fig. 6a and b indicate the spurious eigenvalues for the singular formulation. Similarly, the same drop locations in Fig. 6d and e indicate the spurious eigenvalues for the hypersingular formulation. The spurious eigenequations for the singular and hypersingular formulation are

$$j_n(ka) = 0 \quad \text{and} \quad (74)$$

$$j'_n(ka) = 0, \quad (75)$$

respectively. It is found that spurious eigenvalues depend on the inner boundary instead of the outer boundary. Finally, we employed the SVD updating document to filter out the spurious eigenvalues. The spurious eigenvalues for singular formulation and hypersingular formulation are extracted as shown in Fig. 6c and f, respectively.

7. Conclusions

Spurious eigenvalues for a concentric sphere were studied analytically and numerically. One example was demonstrated to see how the spurious eigenvalues occur in the concentric sphere. Spurious eigenvalues depend on the inner boundary and are independent of the outer boundary. The trivial outer boundary densities were examined in case of the spurious eigenvalue which is found to be the true eigenvalue for the domain bounded by the inner boundary. The contribution of the work is to show the existence of spurious eigenvalue for a concentric sphere in an analytical manner by using the degenerate kernels and the spherical harmonics.

Acknowledgements

The authors wish to thank the support from the Ministry of Economic Affairs of Republic of China under contract 98-EC-17-A-05-S2-0143 for this paper.

Appendix A

	$U(s, x)$ and $\int_B U(s, x)t(s)dB(s)$	$T(s, x)$ and $\int_B T(s, x)u(s)dB(s)$
Degenerate kernel	$U(s, x) = \begin{cases} U^i(s, x) = ik \sum_{n=0}^{\infty} (2n+1) \sum_{m=0}^n \varepsilon_m \frac{(n-m)!}{(n+m)!} \cos(m(\phi - \bar{\phi})) \\ \quad P_n^m(\cos \theta) P_n^m(\cos \bar{\theta}) j_n(k\rho) h_n^{(2)}(k\bar{\rho}), \quad \bar{\rho} \geq \rho, \\ U^e(s, x) = ik \sum_{n=0}^{\infty} (2n+1) \sum_{m=0}^n \varepsilon_m \frac{(n-m)!}{(n+m)!} \cos(m(\phi - \bar{\phi})) \\ \quad P_n^m(\cos \theta) P_n^m(\cos \bar{\theta}) j_n(k\bar{\rho}) h_n^{(2)}(k\rho), \quad \rho > \bar{\rho}. \end{cases}$	$T(s, x) = \begin{cases} T^i(s, x) = ik^2 \sum_{n=0}^{\infty} (2n+1) \sum_{m=0}^n \varepsilon_m \frac{(n-m)!}{(n+m)!} \cos(m(\phi - \bar{\phi})) \\ \quad P_n^m(\cos \theta) P_n^m(\cos \bar{\theta}) j_n(k\rho) h_n^{(2)}(k\bar{\rho}), \quad \bar{\rho} > \rho, \\ T^e(s, x) = ik^2 \sum_{n=0}^{\infty} (2n+1) \sum_{m=0}^n \varepsilon_m \frac{(n-m)!}{(n+m)!} \cos(m(\phi - \bar{\phi})) \\ \quad P_n^m(\cos \theta) P_n^m(\cos \bar{\theta}) j_n(k\bar{\rho}) h_n^{(2)}(k\rho), \quad \rho > \bar{\rho}. \end{cases}$
Orthogonal process	$\begin{cases} \int_0^{2\pi} \int_0^\pi ik \sum_{n=0}^{\infty} (2n+1) \sum_{m=0}^n \varepsilon_m \frac{(n-m)!}{(n+m)!} \cos(m(\phi - \bar{\phi})) \\ \quad P_n^m(\cos \theta) P_n^m(\cos \bar{\theta}) j_n(k\rho) h_n^{(2)}(k\bar{\rho}) \\ \quad P_n^m(\cos \bar{\theta}) \cos(m\bar{\phi}) \bar{\rho}^2 \sin(\bar{\theta}) d\bar{\theta} d\bar{\phi} \\ = 4\pi k i \bar{\rho}^2 j_n(k\rho) h_n^{(2)}(k\bar{\rho}) P_n^m(\cos \theta) \cos(m\phi), \quad \bar{\rho} \geq \rho, \\ \int_0^{2\pi} \int_0^\pi ik \sum_{n=0}^{\infty} (2n+1) \sum_{m=0}^n \varepsilon_m \frac{(n-m)!}{(n+m)!} \cos(m(\phi - \bar{\phi})) \\ \quad P_n^m(\cos \theta) P_n^m(\cos \bar{\theta}) j_n(k\bar{\rho}) h_n^{(2)}(k\rho) \\ \quad P_n^m(\cos \bar{\theta}) \cos(m\bar{\phi}) \bar{\rho}^2 \sin(\bar{\theta}) d\bar{\theta} d\bar{\phi} \\ = 4\pi k i \bar{\rho}^2 j_n(k\bar{\rho}) h_n^{(2)}(k\rho) P_n^m(\cos \theta) \cos(m\phi), \quad \bar{\rho} < \rho. \end{cases}$	$\begin{cases} \int_0^{2\pi} \int_0^\pi ik^2 \sum_{n=0}^{\infty} (2n+1) \sum_{m=0}^n \varepsilon_m \frac{(n-m)!}{(n+m)!} \cos(m(\phi - \bar{\phi})) \\ \quad P_n^m(\cos \theta) P_n^m(\cos \bar{\theta}) j_n(k\rho) h_n^{(2)}(k\bar{\rho}) \\ \quad P_n^m(\cos \bar{\theta}) \cos(m\bar{\phi}) \bar{\rho}^2 \sin(\bar{\theta}) d\bar{\theta} d\bar{\phi} \\ = 4\pi k^2 i \bar{\rho}^2 j_n(k\rho) h_n^{(2)}(k\bar{\rho}) P_n^m(\cos \theta) \cos(m\phi), \quad \bar{\rho} > \rho, \\ \int_0^{2\pi} \int_0^\pi ik^2 \sum_{n=0}^{\infty} (2n+1) \sum_{m=0}^n \varepsilon_m \frac{(n-m)!}{(n+m)!} \cos(m(\phi - \bar{\phi})) \\ \quad P_n^m(\cos \theta) P_n^m(\cos \bar{\theta}) j_n(k\bar{\rho}) h_n^{(2)}(k\rho) \\ \quad P_n^m(\cos \bar{\theta}) \cos(m\bar{\phi}) \bar{\rho}^2 \sin(\bar{\theta}) d\bar{\theta} d\bar{\phi} \\ = 4\pi k^2 i \bar{\rho}^2 j_n(k\bar{\rho}) h_n^{(2)}(k\rho) P_n^m(\cos \theta) \cos(m\phi), \quad \bar{\rho} < \rho. \end{cases}$

(continued on next page)

Appendix A (continued)

	$U(s, x)$ and $\int_B U(s, x) t(s) dB(s)$	$T(s, x)$ and $\int_B T(s, x) u(s) dB(s)$
Limit $\rho \rightarrow \bar{\rho}$	$\begin{cases} 4\pi k i \bar{\rho}^2 j_n(k\bar{\rho}) h_n^{(2)}(k\bar{\rho}) P_n^m(\cos \theta) \cos(m\phi), & \bar{\rho} \geq \rho, \\ 4\pi k i \bar{\rho}^2 j_n(k\bar{\rho}) h_n^{(2)}(k\bar{\rho}) P_n^m(\cos \theta) \cos(m\phi), & \bar{\rho} < \rho. \end{cases}$ (Continuous for $\bar{\rho}^- < \rho < \bar{\rho}^+$)	$\begin{cases} 4\pi k^2 i \bar{\rho}^2 j_n(k\bar{\rho}) h_n^{(2)}(k\bar{\rho}) P_n^m(\cos \theta) \cos(m\phi), & \bar{\rho} > \rho, \\ 4\pi k^2 i \bar{\rho}^2 j_n(k\bar{\rho}) h_n^{(2)}(k\bar{\rho}) P_n^m(\cos \theta) \cos(m\phi), & \bar{\rho} < \rho. \end{cases}$ (Jump for $\bar{\rho}^- < \rho < \bar{\rho}^+$ is $4\pi j_n(k\bar{\rho}) j_n'(k\bar{\rho}) \sum_{n=0}^{\infty} \sum_{m=0}^n P_n^m(\cos \theta) \cos(m\phi)$)
	$L(s, x)$ and $\int_B L(s, x) t(s) dB(s)$	$M(s, x)$ and $\int_B M(s, x) u(s) dB(s)$
Degenerate kernel	$L(s, x) = \begin{cases} L^i(s, x) = ik^2 \sum_{n=0}^{\infty} (2n+1) \sum_{m=0}^n \varepsilon_m \frac{(n-m)!}{(n+m)!} \cos(m(\phi - \bar{\phi})) \\ P_n^m(\cos \theta) P_n^m(\cos \bar{\theta}) j_n'(k\rho) h_n^{(2)}(k\bar{\rho}), & \bar{\rho} > \rho, \\ L^e(s, x) = ik^2 \sum_{n=0}^{\infty} (2n+1) \sum_{m=0}^n \varepsilon_m \frac{(n-m)!}{(n+m)!} \cos(m(\phi - \bar{\phi})) \\ P_n^m(\cos \theta) P_n^m(\cos \bar{\theta}) j_n(k\bar{\rho}) h_n^{(2)}(k\rho), & \rho > \bar{\rho}. \end{cases}$	$M(s, x) = \begin{cases} M^i(s, x) = ik^3 \sum_{n=0}^{\infty} (2n+1) \sum_{m=0}^n \varepsilon_m \frac{(n-m)!}{(n+m)!} \cos(m(\phi - \bar{\phi})) \\ P_n^m(\cos \theta) P_n^m(\cos \bar{\theta}) j_n'(k\rho) h_n^{(2)}(k\bar{\rho}), & \bar{\rho} \geq \rho, \\ M^e(s, x) = ik^3 \sum_{n=0}^{\infty} (2n+1) \sum_{m=0}^n \varepsilon_m \frac{(n-m)!}{(n+m)!} \cos(m(\phi - \bar{\phi})) \\ P_n^m(\cos \theta) P_n^m(\cos \bar{\theta}) j_n'(k\bar{\rho}) h_n^{(2)}(k\rho), & \rho > \bar{\rho}. \end{cases}$
Orthogonal process	$\begin{cases} \int_0^{2\pi} \int_0^\pi ik^2 \sum_{n=0}^{\infty} (2n+1) \sum_{m=0}^n \varepsilon_m \frac{(n-m)!}{(n+m)!} \cos(m(\phi - \bar{\phi})) \\ P_n^m(\cos \theta) P_n^m(\cos \bar{\theta}) j_n'(k\rho) h_n^{(2)}(k\bar{\rho}) \\ P_n^m(\cos \bar{\theta}) \cos(m\bar{\phi}) \bar{\rho}^2 \sin(\bar{\theta}) d\bar{\theta} d\bar{\phi} \\ = 4\pi k^2 i \bar{\rho}^2 j_n'(k\rho) h_n^{(2)}(k\bar{\rho}) P_n^m(\cos \theta) \cos(m\phi), & \bar{\rho} > \rho, \\ \int_0^{2\pi} \int_0^\pi ik^2 \sum_{n=0}^{\infty} (2n+1) \sum_{m=0}^n \varepsilon_m \frac{(n-m)!}{(n+m)!} \cos(m(\phi - \bar{\phi})) \\ P_n^m(\cos \theta) P_n^m(\cos \bar{\theta}) j_n(k\bar{\rho}) h_n^{(2)}(k\rho) \\ P_n^m(\cos \bar{\theta}) \cos(m\bar{\phi}) \bar{\rho}^2 \sin(\bar{\theta}) d\bar{\theta} d\bar{\phi} \\ = 4\pi k^2 i \bar{\rho}^2 j_n(k\bar{\rho}) h_n^{(2)}(k\rho) P_n^m(\cos \theta) \cos(m\phi), & \bar{\rho} < \rho. \end{cases}$	$\begin{cases} \int_0^{2\pi} \int_0^\pi ik^3 \sum_{n=0}^{\infty} (2n+1) \sum_{m=0}^n \varepsilon_m \frac{(n-m)!}{(n+m)!} \cos(m(\phi - \bar{\phi})) \\ P_n^m(\cos \theta) P_n^m(\cos \bar{\theta}) j_n'(k\rho) h_n^{(2)}(k\bar{\rho}) \\ P_n^m(\cos \bar{\theta}) \cos(m\bar{\phi}) \bar{\rho}^2 \sin(\bar{\theta}) d\bar{\theta} d\bar{\phi} \\ = 4\pi k^3 i \bar{\rho}^2 j_n'(k\rho) h_n^{(2)}(k\bar{\rho}) P_n^m(\cos \theta) \cos(m\phi), & \bar{\rho} \geq \rho, \\ \int_0^{2\pi} \int_0^\pi ik^3 \sum_{n=0}^{\infty} (2n+1) \sum_{m=0}^n \varepsilon_m \frac{(n-m)!}{(n+m)!} \cos(m(\phi - \bar{\phi})) \\ P_n^m(\cos \theta) P_n^m(\cos \bar{\theta}) j_n'(k\bar{\rho}) h_n^{(2)}(k\rho) \\ P_n^m(\cos \bar{\theta}) \cos(m\bar{\phi}) \bar{\rho}^2 \sin(\bar{\theta}) d\bar{\theta} d\bar{\phi} \\ = 4\pi k^3 i \bar{\rho}^2 j_n'(k\bar{\rho}) h_n^{(2)}(k\rho) P_n^m(\cos \theta) \cos(m\phi), & \bar{\rho} < \rho. \end{cases}$
Limit $\rho \rightarrow \bar{\rho}$	$\begin{cases} 4\pi k^2 i \bar{\rho}^2 j_n'(k\bar{\rho}) h_n^{(2)}(k\bar{\rho}) P_n^m(\cos \theta) \cos(m\phi), & \bar{\rho} > \rho, \\ 4\pi k^2 i \bar{\rho}^2 j_n(k\bar{\rho}) h_n^{(2)}(k\bar{\rho}) P_n^m(\cos \theta) \cos(m\phi), & \bar{\rho} < \rho. \end{cases}$ (Jump for $\bar{\rho}^- < \rho < \bar{\rho}^+$ is $4\pi j_n(k\bar{\rho}) j_n'(k\bar{\rho}) \sum_{n=0}^{\infty} \sum_{m=0}^n P_n^m(\cos \theta) \cos(m\phi)$)	$\begin{cases} 4\pi k^3 i \bar{\rho}^2 j_n'(k\bar{\rho}) h_n^{(2)}(k\bar{\rho}) P_n^m(\cos \theta) \cos(m\phi), & \bar{\rho} \geq \rho, \\ 4\pi k^3 i \bar{\rho}^2 j_n(k\bar{\rho}) h_n^{(2)}(k\bar{\rho}) P_n^m(\cos \theta) \cos(m\phi), & \bar{\rho} < \rho. \end{cases}$ (Continuous for $\bar{\rho}^- < \rho < \bar{\rho}^+$)

References

- [1] Chen IL, Chen JT, Lee WM, Kao SK. Computer assisted proof of spurious eigensolution for annular and eccentric membranes. *J Mar Sci Technol* 2009; in press.
- [2] Ali A, Rajakumar C, Yunus SM. Advances in acoustic eigenvalue analysis using boundary element method. *Comput Struct* 1995;56(5):837–47.
- [3] Winkler JR, Davies JB. Elimination of spurious modes in finite element analysis. *J Comput Phys* 1984;56:1–14.
- [4] Greenberg MD. *Advanced engineering mathematics*. New Jersey: Prentice-Hall; 1998.
- [5] Fujiwara H. High-accurate numerical computation with multiple-precision arithmetic and spectral method, unpublished report; 2007.
- [6] Zhao S. On the spurious solutions in the high-order finite difference methods for eigenvalue problems. *Comput Methods Appl Mech Eng* 2007;196: 5031–46.
- [7] Kuo SR, Chen JT, X Huang C. Analytical study and numerical experiments for true and spurious eigensolutions of a circular cavity using the real-part dual BEM. *Int J Numer Methods Eng* 2000;48:1401–22.
- [8] Chen JT, Wong FC. Analytical derivations for one-dimensional eigenproblems using dual boundary element method and multiple reciprocity method. *Eng Anal Bound Elem* 1997;20:25–33.
- [9] Chen JT, Wong FC. Dual formulation of multiple reciprocity method for the acoustic mode of a cavity with a thin partition. *J Sound Vib* 1998;217(1): 75–95.
- [10] Yehi W, Chen JT, Chen KH, Wong FC. A study on the multiple reciprocity method and complex-valued formulation for the Helmholtz equation. *Adv Eng Soft* 1998;29(1):1–6.
- [11] Yehi W, Chen JT, Chang CM. Applications of dual MRM for determining the natural frequencies and natural modes of an Euler-Bernoulli beam

- using the singular value decomposition method. *Eng Anal Bound Elem* 1999;23:339–60.
- [12] Yehi W, Chang JR, Chang CM, Chen JT. Applications of dual MRM for determining the natural frequencies and natural modes of a rod using the singular value decomposition method. *Adv Eng Soft* 1999;30:459–68.
- [13] Chen JT, Kuo SR, Chung IL, Huang CX. Study on the true and spurious eigensolutions of two-dimensional cavities using the multiple reciprocity method. *Eng Anal Bound Elem* 2003;27:655–70.
- [14] Chen JT, Lin JH, Kuo SR, Chyuan SW. Boundary element analysis for the Helmholtz eigenvalue problems with a multiply connected domain. *Proc Roy Soc A* 2001;457:2521–46.
- [15] Chen JT, Liu LW, Hong HK. Spurious and true eigensolutions of Helmholtz BIEs and BEMs for a multiply-connected problem. *Proc Roy Soc A* 2003;459:1891–925.
- [16] Chen JT, Chen IL, Chen KH. Treatment of rank deficiency in acoustics using SVD. *J Comput Acoust* 2006;14(2):157–83.
- [17] Tsai CC, Young DL, Chen CW, Fan CN. The method of fundamental solutions for eigenproblems in the domains with and without interior holes. *Proc Roy Soc A* 2006;462:1443–66.
- [18] Chen JT, Lee CF, Lin SY. A new point of view for the polar decomposition using singular value decomposition. *Int J Comput Numer Anal* 2002;2(3): 257–64.
- [19] Chen JT, Shen WC, Wu AC. Null-field integral equations for stress field around circular holes under anti-plane shear. *Eng Anal Bound Elem* 2006;30(3): 205–17.
- [20] Chen JT, Chen PY. A semi-analytical approach for stress concentration of cantilever beams with holes under bending. *J Mech* 2007;23(3):211–21.
- [21] Chen JT, Chen CT, Chen PY, Chen IL. A semi-analytical approach for radiation and scattering problems with circular boundaries. *Comput Methods Appl Mech Eng* 2007;196:2751–64.